Supporting Information

Cox et al. 10.1073/pnas.1117275109

SI Materials and Methods

Constructs for Expression of Recombinant Proteins. *Escherichia coli* BL21 (λDE3; pET-28:*fusB*) (1) was used for expression of FusB. A construct for overexpression of *Staphylococcus aureus* EF-G was generated by PCR amplification of *fusA* from SH1000 (2) using oligonucleotide primers FusAU and FusAL (Table S2) and ligated into pET-3. The *fusC* gene was PCR amplified from MSSA476 (3) using primers FusCU and FusCL (Table S2) and ligated into a modified pET-19b expression vector (Novagen) encoding an N-terminal His-tag followed by a Tobacco etch virus protease recognition site. Constructs for the expression of fragments 1–4 of EF-G were generated by PCR amplification and ligation into pET-29. Recombinant proteins were overexpressed in *E. coli* BL21 Rosetta 2 (λDE3; Novagen) or BL21 Gold (λDE3; Agilent Technologies).

Analytical Gel Filtration Chromatography. Analytical gel filtration chromatography was carried out at 4 °C using a S75 pg (16/60) prepacked column (GE Healthcare). Purified EF-G or fragments of EF-G (2 mg) were incubated with FusB or FusC (10 mg) in a final volume of 2 mL for 1 h at 4 °C. Samples were eluted in running buffer at a flow rate of 0.5 mL/min, and analyzed by SDS/PAGE.

Crystallization of FusC and Data Collection. Crystals of FusC were grown from hanging drops using the vapor diffusion method. Drops comprised 1 μL of FusC at a concentration of 20 mg/mL, and 1 μL reservoir solution containing 0.2 M ammonium acetate, 0.1 M Tris·HCl (pH 8.0), and 20% (wt/vol) PEG 3350 were equilibrated above the reservoir solution at 4 °C. Crystals were frozen in nitrogen after being transferred through the mother liquor containing 25% (vol/vol) ethylene glycol.

X-ray diffraction data were collected at Diamond Light Source beam line I02. Data were indexed and integrated using XDS (4) and reduced with SCALA (5). The FusC structure was solved using single-wavelength anomalous data (SAD) (6). To determine the wavelengths around the zinc absorption edge for SAD data collection, X-ray fluorescence scans were obtained and analyzed using the program CHOOCH (7). Zinc sites were determined using SHELX (8), and initial phases from PHASER (9) were improved using RESOLVE (10, 11). Density-modified phases were provided to ARP/warp (12) for automatic chain tracing. The initial model was improved through iterative rounds of model rebuilding in COOT (13) and refinement with REFMAC (14), or simulated annealing in PHENIX (15). The MolProbity Web service (16) was used to validate the refined FusC structure and produced a clash score within the 84th percentile and overall MolProbity score in the 90th percentile. Data collection and final refinement statistics are shown in Table S1.

NMR Spectroscopy. NMR experiments were performed with perdeuterated 0.3 mM ^{15}N- and ^{13}C-labeled His-tagged FusB in running buffer containing 90% H_2O/10% D_2O. For analysis of the FusB·EF-G_{C3} complex, perdeuterated ^{15}N-labeled FusB was saturated with unlabeled EF-G_{C3} and the complex purified by gel filtration chromatography. Spectra were recorded at 25 °C on a Varian Inova 600-MHz spectrometer with a room temperature probe, or a Varian Inova 750-MHz spectrometer with a cryogenic probe.

Backbone assignments of FusB were obtained from analysis of HNCA, HNCO, HN(CO)CA, HN(CA)CO, and HN(CA)CB spectra (all experiments used TROSY modifications and, where required, deuterium decoupling) (17). Data were processed in NMRPipe (18) before assignment and measurement of chemical shift oxides and shift mapping by CCPN analysis (19). The program MAPPER 2.0 was used to place backbone fragments (20). Chemical shift indexing (21) was used to determine the secondary structure of FusB from the shifts of ^{1}H and ^{13}C nuclei. Conservative chemical shift differences between the ^{1}H -^{15}N spectra for FusB and FusB·EF-G_{C3} were calculated by finding the closest peak in the FusB·EF-G_{C3} spectrum to the assigned peaks in the FusB spectrum using the metric $\Delta = [(\delta^{15}N_{FusB/FusB-C3}) + (5 \times \delta^{1}H_{FusB/FusB-C3})^{2}]^{0.5}$ (22). Shift differences for which $\Delta > 0.6$ ppm were considered significant and indicated residues involved in forming the FusB·EF-G_{C3} interface. Spectra were referenced in the ^{1}H dimension using the methyl protons of D6-dimethyl-2-silapentane-5-sulfonic acid. ^{13}C and ^{15}N dimensions were indirectly referenced (23).

1. O'Neill AJ, Chopra I (2006) Molecular basis of *fusB*-mediated resistance to fusidic acid in *Staphylococcus aureus*. *Mol Microbiol* 59:664–676.
2. Horsburgh MJ, et al. (2002) sigmaB modulates virulence determinant expression and stress resistance: Characterization of a functional *rsbU* strain derived from *Staphylococcus aureus* 8325-4. *J Bacteriol* 184:5457–5467.
3. Holden MT, et al. (2004) Complete genomes of two clinical *Staphylococcus aureus* strains: Evidence for the rapid evolution of virulence and drug resistance. *Proc Natl Acad Sci USA* 101:9786–9791.
4. Kabsch W (2010) Xds. *Acta Crystallogr D Biol Crystallogr* 66:125–132.
5. Evans PR (1997) SCALA, a continuous scaling program. *Joint CCP4 and ESF-EACBM Newsletter on Protein Crystallography* 33:22–24.
6. Hendrickson WA (1991) Determination of macromolecular structures from anomalous diffraction of synchrotron radiation. *Science* 254:51–58.
7. Evans G (2005) CHOOCH—automatic analysis of fluorescence scans and determination of optimal X-ray wavelengths for MAD and SAD. *CCP4 Newsletter on Protein Crystallography* 42:33–37.
8. Sheldrick GM (2008) A short history of SHELX. *Acta Crystallogr A* 64:112–122.
9. McCoy AJ, et al. (2007) Phaser crystallographic software. *J Appl Cryst* 40:658–674.
10. Terwilliger TC (2000) Maximum-likelihood density modification. *Acta Crystallogr D Biol Crystallogr* 56:965–972.
11. Terwilliger TC (2003) SOLVE and RESOLVE: Automated structure solution and density modification. *Methods Enzymol* 374:22–37.
12. Langer G, Cohen SX, Lamzin VS, Perrakis A (2008) Automated macromolecular model building for X-ray crystallography using ARP/wARP version 7. *Nat Protoc* 3:1171–1179.
13. Emsley P, Lohkamp B, Scott WG, Cowtan K (2010) Features and development of Coot. *Acta Crystallogr D Biol Crystallogr* 66:486–501.
14. Skubák P, Murshudov GN, Pannu NS (2004) Direct incorporation of experimental phase information in model refinement. *Acta Crystallogr D Biol Crystallogr* 60(Pt 12 Pt 1):2196–2201.
15. Adams PD, et al. (2010) PHENIX: A comprehensive Python-based system for macromolecular structure solution. *Acta Crystallogr D Biol Crystallogr* 66:213–221.
16. Chen VB, et al. (2010) MolProbity: All-atom structure validation for macromolecular crystallography. *Acta Crystallogr D Biol Crystallogr* 66:12–21.
17. Sattler M, Schleucher J, Griesinger C (1999) Heteronuclear multidimensional NMR experiments for the structure determination of proteins in solution employing pulsed field gradients. *Prog Nucl Mag Res Sp* 34:93–158.
18. Delaglio F, et al. (1995) NMRPipe: A multidimensional spectral processing system based on UNIX pipes. *J Biomol NMR* 6:277–293.
19. Vranken WF, et al. (2005) The CCPN data model for NMR spectroscopy: Development of a software pipeline. *Proteins* 59:687–696.
20. Güntert P, Salzmann M, Braun D, Wüthrich K (2000) Sequence-specific NMR assignment of proteins by global fragment mapping with the program MAPPER. *J Biomol NMR* 18:129–137.
21. Wishart DS, Sykes BD (1994) The 13C chemical-shift index: A simple method for the identification of protein secondary structure using 13C chemical-shift data. *J Biomol NMR* 4:171–180.
22. Williamson RA, Carr MD, Frenkiel TA, Feeney J, Freedman RB (1997) Mapping the binding site for matrix metalloproteinase on the N-terminal domain of the tissue inhibitor of metalloproteinases-2 by NMR chemical shift perturbation. *Biochemistry* 36:13882–13889.
23. Markley JL, et al. (1998) Recommendations for the presentation of NMR structures of proteins and nucleic acids—IUPAC-IUBMB-IUPAB Inter-Union Task Group on the standardization of data bases of protein and nucleic acid structures determined by NMR spectroscopy. *Eur J Biochem* 256:1–15.

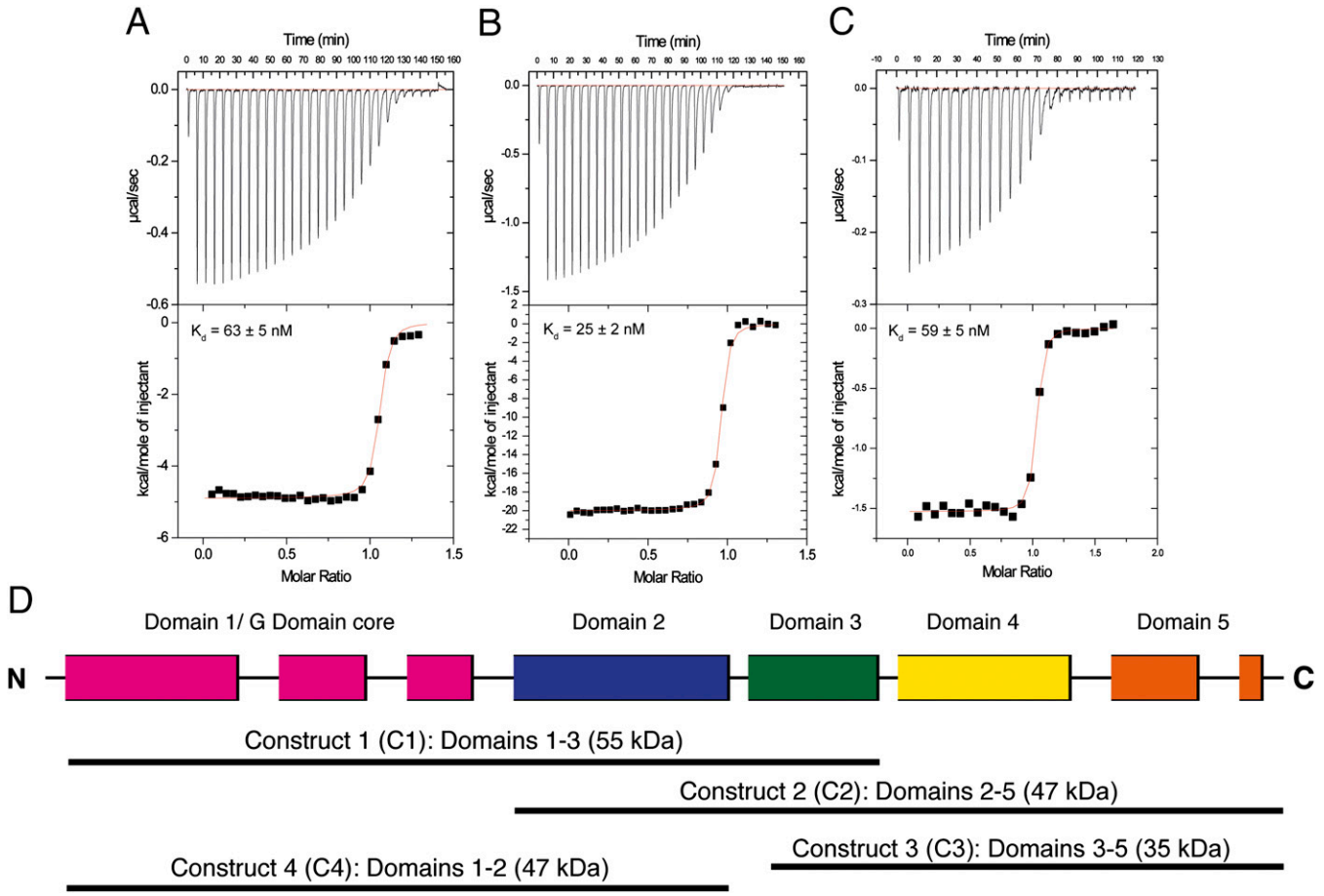

Fig. S1. Analysis of binding of whole and partial EF-G to FusB-type proteins by isothermal titration calorimetry. Shown are representative data for titrations of (*A*) EF-G with FusB, (*B*) EF-G with FusC, and (*C*) EF-G_{C3} (domains 3–5 of EF-G) with FusB. (*D*) Schematic showing the domain architecture of EF-G, EF-G_{C3}, and other EF-G fragments used in this study.

```
                                    150                                              199
             S. aureus YP_042173    KVKGFCKICN QESDTSLFLN KTKHNKSSGT YTKKGDYICY DSFKCNQNLD
             S. aureus AAL12234     VVKGFCTICN KESNVSLFMK KSKTN.SDGQ YVKKGDYICR DSIHCNKQLT
     S. saprophyticus YP_302255     TVKSFCSICN KESRVALFMR KTRTG.NDGQ YTKKGDYICF DSTLCNHQIS
            E. faecium ZP_06674445  INKGICAICQ KTSNVSLFLS TTKAG.SDGT YTKKGNYICH DSDQCNQQLT
            L. innocua NP_470072    IQKGVCSICQ THSKVSLFMA KTKSS.SDGV YTTNGNYICY DSDVCNEQIK
W. paramesenteroides ZP_04783961    VVKGYCAICH HEENVSMFLA LNKRR.GDGR YTKKGNYICV DSLQCNRNLH
     E. casseliflavus ZP_05645644   VKKGICPLCQ HEGNVSMFLS LTKSN.GDGT YTKRGNYICR DSQRCNQQME
         L. plantarum ZP_07078794   TVKGVCAICQ TIGNVALFMS TTKSS.GLGP YTRNGNYICR DSNQCNRQLT
             B. cereus NP_978243    NKKSICSLCH GHEEVGMFLV EIKGD.IPGT FVKKGNYICK DGVACNQNMK
            L. lactis YP_003354811  .MKNICAICQ KTSIVTQFLA TTKRG.ADGT YTKNGTYICL DSEQCNQQIQ
                        Consensus   ..KgiC.iCq ..s.v..F$. .tK....dGt %tkkGnYIC. Ds..CNq#..
```

Fig. S2. Sequence alignment of the conserved C4 zinc finger within FusB homologs. The source and GenBank accession number of each protein are shown. The K-x_2-C-x_2-C-x_8-F-x_4-K-x_4-G-x_5-G-x-YIC-x-D-x_3-CN motif (colored red) is highly conserved. Numbering corresponds to the FusC amino acid sequence (YP_042173).

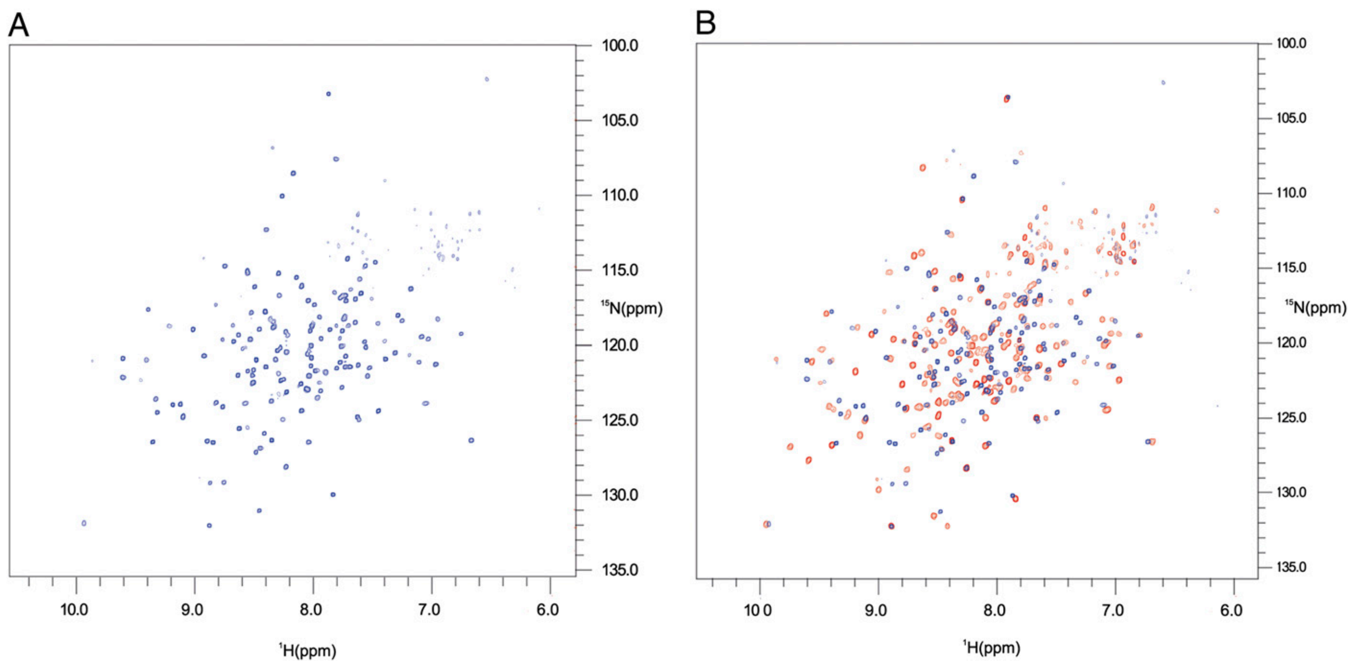

Fig. S3. Trosy ^{1}H-^{5}N heteronuclear single-quantum coherence (HSQC) spectra of (*A*) ^{15}N-FusB and (*B*) ^{15}N-FusB bound to unlabeled EF-G_{C3}. Spectra from the free ^{15}N-FusB protein are shown in blue, and spectra of the ^{15}N-FusB·EF-G_{C3} complex in red (overlaid with ^{1}H-^{5}N HSQC spectra of free ^{15}N-FusB).

Table S1. Crystallographic data collection, phasing, and refinement statistics

	FusC native	FusC Zn SAD
Data collection		
X-ray source	Diamond Light Source beamline I03	Diamond Light Source beamline I02
Wavelength, Å	0.97	1.28
Space group	$P2_1$	$P2_1$
Unit cell parameters	a = 34.15 Å	a = 33.85 Å
	b = 109.61 Å	b = 109.79 Å
	c = 61.15 Å	c = 61.11 Å
	$\alpha = \gamma = 90°$	$\alpha = \gamma = 90°$
	$\beta = 101.7°$	$\beta = 102.3°$
Resolution, Å	40.4–2.1	28.2–2.5
Unique reflections	25,179	15,114
Total reflections	186,175	111,979
Completeness (%)	98.0 (97.6)	99.8 (100.0)
Multiplicity	7.4 (7.3)	7.4 (7.5)
I/σ*	15.4 (2.6)	36.2 (8.3)
R_{merge}*,†	0.072 (0.771)	0.032 (0.217)
R_{pim}*,‡	0.028 (0.30)	0.018 (0.094)
Phasing statistics		
No. of zinc sites		2
FoM§; centric, acentric, overall		0.089, 0.432, 0.408
Refinement statistics		
Resolution range, Å	15–2.1	
R_{work}, R_{free}¶,‖	0.2133, 0.2857	
No. of atoms: protein; water/ion; other	6,974; 563; 78	
Rmsd bonds, Å	0.0089	
Rmsd angle, °	1.1095	
Average B factors	39.89	
MolProbity: clash score, overall score	84th, 90th percentile	

*Values for the highest-resolution shell are given in parentheses.
†$R_{merge} = \sum_{hkl} \sum_i |I_i(hkl) - \langle I(hkl)\rangle| / \sum_{hkl} \sum_i I_i(hkl)$, where $I_i(hkl)$ is the intensity of reflection hkl and $\sum_i$ is the sum over all i measurements of reflection hkl.
‡$R_{p.i.m} = \sum_{hkl} [1/(n_{hkl} - 1)]^{1/2} \sum_i |I_i(hkl) - \langle I(hkl)\rangle| / \sum_{hkl} \sum_i I_i(hkl)$, where n_{hkl} is the number of observations of reflection hkl.
§Figure of merit.
¶R factor $R_{work} = \sum_{hkl} ||F_{obs}| - |F_{calc}|| / \sum_{hkl} |F_{obs}|$, where F_{obs} and F_{calc} are the observed and calculated structure factors, respectively.
‖R_{free} is the R factor calculated over a subset of the data (5.1%) that were excluded from refinement.

Table S2. Oligonucleotide primers used in this study

Designation	Sequence (5′–3′)
FusCU	GAATATCATATGAATAAAATAGAAGTGT
FusCL	GGCCCTCGAGATCTATTTTATTTTAACAATAA
FusAU	AGAAAAAACATATGGCTAGAGAATTTTCATTAG
FusAL	TATTGGATCCAGGCTAGTTAGTGGTGGTGGTGGTGTTCGCCTTTATTTTTCTTGATAATATC
Construct1U	AGAAAAAACATATGGCTAGAGAATTT
Construct1L	GATGTCTCGAGATATGAAACCATTGGAGCA
Construct2U	AGACGTTCATATGATTATTGGTCACCGT
Construct2L	AACAAGTTCTCGAGTTCACCTTTATTTTTC
Construct3U	CTTCGAACATATGGAATTCCCAGAGCCA
Construct3L	AACAAGTTCTCGAGTTCACCTTTATTTTTC
Construct4U	AGAAAAAACATATGGCTAGAGAATTT
Construct4L	TGGCTCCTCGAGTTCCATTGATTCCAAGA

Restriction sites are shown underlined.